

Effect of Corrosion Product Concentration on Thermal Conductivity of Crud

Yunju Lee, Junhyuk Ham, Seung Chang Yoo, Dae Hyeon Park, Ji Hyun Kim*

Department of Nuclear Engineering, College of Engineering, Ulsan National Institute of Science and Technology (UNIST)

*Corresponding author: kimjh@unist.ac.kr

1. Introduction

In Nuclear Power Plant (NPP), Corrosion Product Related Deposit (crud, or called Chalk River Unidentified Deposits) is formed by sub-cooled boiling on the upper part of fuel cladding. The corrosion products provoke serious economical and safety issues, which related with boron accumulation and radioactivation of itself. [1-4] The crud deposition and boron accumulation are influenced by chemical and thermal-hydraulic behavior of water near fuel cladding surface. [5] Thus, to predict the effect of crud deposition, crud deposition mechanism should be investigated, considering chemical and thermal-hydraulic condition. While crud thickness and structure are known to be dependent on the heat flux condition of fuel cladding surface and the metal ion concentration of coolant, few study was conducted for the microstructure changes of crud in different metal ion conditions.

To investigate crud deposition on fuel cladding under various water chemistry condition in simulated Pressurized Water Reactor (PWR) primary water, the experimental facility has been set up. In previous study, effect of heat flux on crud structure and chemistry was examined for high metal ion concentration condition. In this study, to investigate effect of metal ion concentration condition on crud formation, crud deposition experiment was conducted for two different metal ion concentration. The specimens were observed by Scanning Electron Microscopy (SEM) with Focused Ion Beam (FIB) instrument. The chemistry and microstructure of crud specimens are examined by Energy Dispersive X-ray Spectroscopy (EDS).

2. Experimental Methods

2.1. Experimental condition

To simulate the crud deposition at reactor core, three major conditions should be satisfied: existence of corrosion product in the primary water, sub-cooled boiling at cladding surface, and dissolved boron and lithium species in the primary water.

Corrosion products, which have been known as source of crud, are formed by structural material of primary coolant system. In PWR, about 80% of primary coolant system surface are composed of nickel alloys and the others are usually stainless steel. Considering corrosion rate and surface composition of the alloys, dissolved Ni/Fe ion rate are calculated to 2. This also well-matched with chemical analysis results of Halden reactors.

The corrosion product is simulated by metal ions such as nickel and iron, which are injected with nickel acetate

and Fe Ethylenediaminetetraacetic acid (EDTA). To accelerate the crud deposition, concentrated metal ion solutions were used.

The proper Ni and Fe ion concentration were assumed to be 100 ppb and 50 ppb, because Ni and Fe ion concentration are limited to maintain under 100 ppb in PWR primary coolant. To simulate 1 cycle (18 month) of NPP operation in 7 days of experiment, Ni 12.5 ppm and Fe 6 ppm solution was prepared. To identify the effect of metal ion concentration on formation of crud, the crud deposition experiment also conducted at 2 times more higher metal ion concentrated solution.

The degree of sub-cooled boiling at fuel cladding specimen was controlled by adjusting the heat flux condition. Because the crud deposition behavior occurs at upper span of the fuel assembly, the experimental conditions was set to simulate the top span of fuel assembly of OPR1000. Heat flux of top span fuel cladding is low (about 150 kW/m²) while the coolant temperature of a top span fuel cladding is high (about 320 °C). Other chemical and thermal conditions are set simulating PWR primary water. Experimental conditions are summarized in **Table 1**.

Table 1. Experimental conditions of crud deposition experiment.

Experimental condition	Low Metal Ion concentration	High Metal Ion concentration
Nickel concentration [ppm]	12.5	25
Iron concentration [ppm]	6	12
Heat flux at specimen [kW/m ²]	150	150
Surface temperature of specimen [°C]	349 ~ 351	357 ~ 365
Average coolant temperature [°C]	318 ~ 330	310 ~ 315
Effective full power day [day]	7	
Length of specimen [mm]	300	
Outer diameter of specimen [mm]	9.5	
Inner diameter of specimen [mm]	8.34	
Pressure [MPa]	15.5	
DH concentration [ppm]	2.7	
DO concentration [ppb]	~ < 5	
pH [ppm]	6.9 ~ 7.4	
Boron concentration [ppm]	1200	
Lithium concentration [ppm]	2.2	

For in-situ surface temperature measurement, a thermocouple is installed at inner surface of the specimen. The test section autoclave is located at test section loop so that high pressure, high temperature and high flow rate conditions were constructed. The cladding specimen was installed at test section autoclave and penetrating the autoclave by using feedthrough fitting so that the specimen can be connected to electrode.

2.2. Analysis strategy

Visual inspection was conducted for the entire specimen to observe macroscopic characteristic of crud deposition behavior. OM images were taken to observe surface of the specimen in macro-scale.

After the visual inspection, microscopic observation was conducted with FIB-SEM instrument. To investigate the axial characteristic of the crud, the specimen is cut in three pieces in axial direction (Top, Middle, Bottom as shown in **Figure 1.**) and SEM was conducted for each specimen.

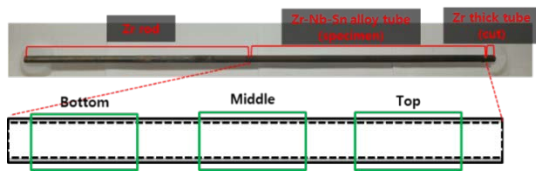


Figure 1. Schematic diagram of a fuel cladding specimen.

During experiment, cladding surface temperature was increased after metal ion injection. This indicate that crud layer, which can be act as heat transfer resistance, is formed. In this paper, effective thermal conductivity of crud was calculated from temperature difference before and after the crud formation. By assuming that bulk coolant temperature and convective heat transfer coefficient of cladding/coolant interface or crud/coolant interface is equal before and after crud deposition, effective thermal conductivity could be calculated by Equation 1.

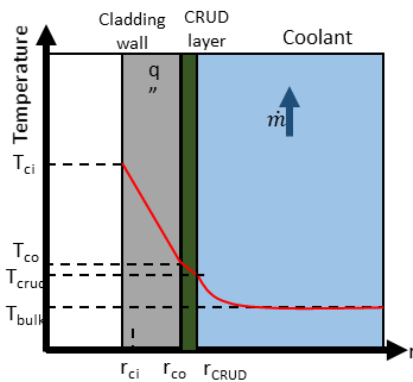


Figure 2. Schematic diagram of temperature change near cladding wall.

$$k_{Crud} = \frac{q'' \pi D_{co}}{A_{crossL}} \cdot \frac{1}{4(T_{co} - T_{Crud})} \left[2r_{co}^2 \ln\left(\frac{r_{co}}{r_{Crud}}\right) + (r_{Crud}^2 - r_{co}^2) \right] \quad (1)$$

3. Results and discussion

3.1. Structural and chemical analysis of crud layer

SEM surface image was taken from top specimen to identify morphology, such as particle size, particle type, porosity and chimney structure (**Figure 3.**). In both specimens, crud layer is mostly composed of few nanometer size particles. And fetal-like-structures are found rarely.

As shown in **Figure 3.** (a), primitive chimney structures were found on the crud layer formed in low metal ion concentration, while fully developed chimney structures were observed on the crud layer formed in high metal ion concentration (**Figure 3.** (b)).

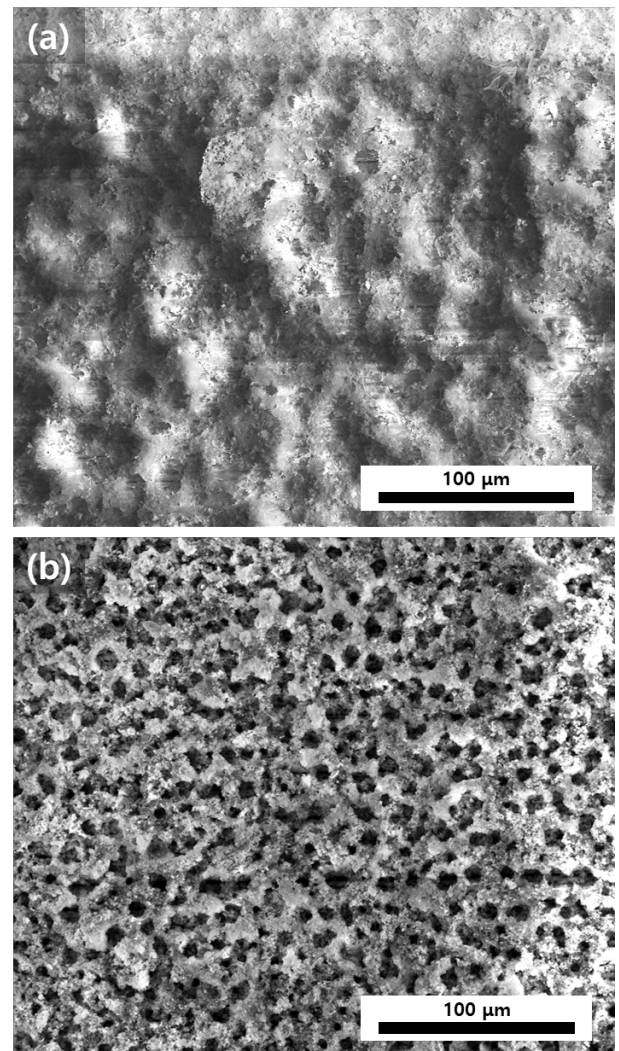


Figure 3. Surface image of crud layer which formed in (a) low metal ion concentration and (b) high metal ion concentration.

Structure of chimney and crud layer were examined using a dual beam FIB-SEM. Cross-section of each specimen was fabricated by FIB in perpendicular to the axial direction of the tube and point EDS was measure in radial direction. EDS location was indicated in crud thickness (Figure 4. and Figure 5.).

Tortuous chimney structure was developed from cladding surface to crud surface in both specimens. Structural characteristics such as porosity, particle size and chimney size of each specimen were similar except thickness. However, chemical compositions of each specimen shows discernible difference at inner crud layer. While Ni/Fe ratio of high metal ion concentration specimen was increase as goes to outward and then reached to 2, Ni/Fe ratio of low metal ion concentration specimen was maintained to 2.

From previous study, which summarized numerous analysis results of crud formed in PWR fuel cladding, Ni-riched crud layer were found at cladding surface which were exposed to more severe temperature condition. [2,3]

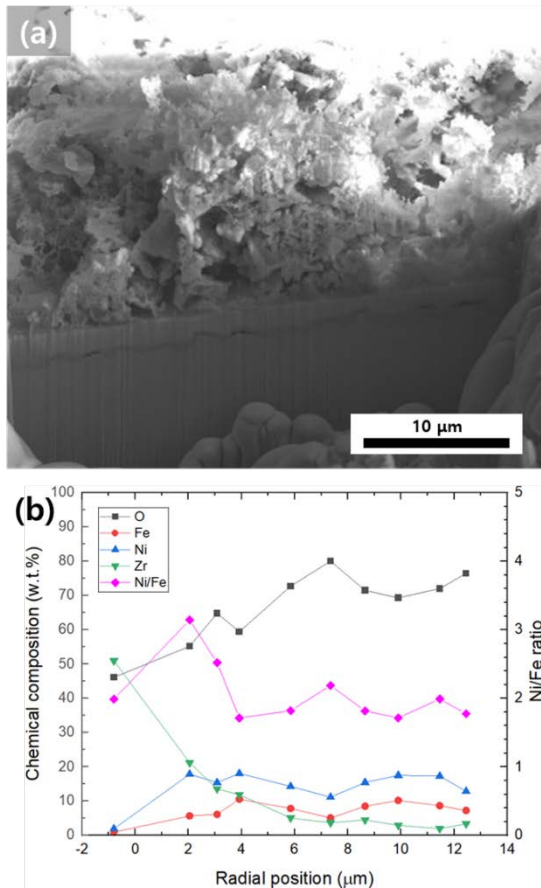


Figure 4. (a) Cross section image and (b) chemical composition of crud layer, which formed in low metal ion concentration.

The cross-section image shows that crud is formed on the rigid ZrO₂ layer. The average thickness of the Zr oxide and crud layer in the FIB spot of top region were summarized in Table 2. Zr oxide was thicker and was

rougher at lower metal ion concentration. This indicate that low metal ion concentration specimen was exposed to more oxidizing condition than high metal ion concentration specimen.

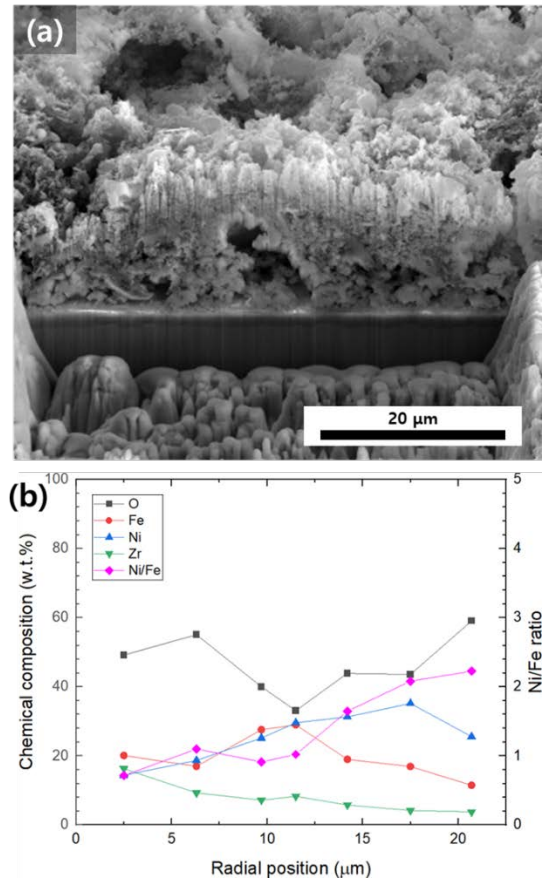


Figure 5. (a) Cross section image and (b) chemical composition of crud layer, which formed in high metal ion concentration.

From the fact that low metal ion concentration specimen has higher Ni/Fe ratio and thicker oxide layer, it can be reasonably concluded that temperature of crud/cladding interface was higher at low metal ion concentration specimen. Despite of above inference, thicker crud layer was deposited in high metal ion concentration.

Table 2. Thickness of Crud and Zr oxide

Thickness	Low Metal Ion concentration	High Metal Ion concentration
Zr oxide	2.24μm (σ=0.547)	1.69μm (σ=0.176)
Crud	11.2μm (σ=4.55)	19.1μm (σ=3.16)

3.2 Effective thermal conductivity of crud layer

Effective thermal conductivity of crud layer was calculated by surface temperature difference before and after the crud deposition experiment (Table 3.).

Although the crud thickness was much thicker at high metal ion concentration, effective thermal conductivity of crud was lower. This can be explained by development stage of chimney structure in each specimen. Diameter of chimney was similar at both specimen while chimney length, which is proportional to crud thickness, is much shorter at low metal ion concentration specimen.

Chimney structure have been known to promote heat transfer between cladding to coolant by provoking Wick boiling. [4] As the short chimney structure are more unfavorable in generating Wick boiling, effective thermal conductivity of crud layer could be lower at low metal ion concentration specimen, which have more primitive chimney structure.

[1] T. Alhashan, M. Elforjani, A. Addali, J. Teixeira, Monitoring of bubble formation during the boiling process using acoustic emission signals, *Int. J. Eng. Res. Sci.* 2(4), 66-72, 2016.
 [2] S. H. Baek, H. -S. Shim, J. G. Kim, D. H. Hur, Visualization and acoustic emission monitoring of nucleate boiling on rough and smooth fuel cladding surfaces at atmospheric pressure, *Nucl. Eng. Des.*, 330, 429-436, 2018.
 [3] C. A. Brett, A. O. Brett, *Electrochemistry*, Oxford Univ. Press, New York, 1994.
 [4] J. Deshon, *Simulated Fuel Crud Thermal Conductivity Measurements Under Pressurized Water Reactor Conditions*, TR-1022896, EPRI, Palo Alto, CA.
 [5] D. Hussey, *PWR Axial Offset Anomaly (AOA) Guidelines*, TR-1008102, EPRI, Palo Alto, CA.

Table 3. Cladding surface temperature change and calculated thermal conductivity of crud

	Low Metal Ion concentration	High Metal Ion concentration
Cladding surface temperature change after crud deposition	3.4 °C	2.4 °C
Calculated effective thermal conductivity	0.00561 W/m-K	0.0224 W/m-K

4. Conclusions

Simulated crud deposition experiments were conducted for different metal ion concentration to investigate the effect of corrosion product concentration on crud deposition and its thermal conductivity.

To identify the relationship between thermal conductivity and structure of crud, each specimen was investigated using SEM and EDS. Effective thermal conductivity of crud was calculated using surface temperature difference before and after the crud deposition experiment.

Through the quantitative comparison, it is known that effective thermal conductivity of crud was lower at low metal ion concentration condition, despite of its thinner crud thickness. By comparing structural characteristic of crud layer, it can be reasonably concluded that developed chimney structure could promote heat transfer in crud far more by actuating Wick boiling behavior than primitive chimney structure.

ACKNOWLEDGEMENT

This work was supported by the Nuclear Safety Research Program through the Korea Foundation Of Nuclear Safety (KoFONS) using the financial resource granted by the Nuclear Safety and Security Commission (NSSC) of the Republic of Korea. (No. 2106022) This study contains the results obtained by using the equipment of UNIST Central Research Facilities (UCRF).

REFERENCES